https://erjm.journals.ekb.eg
ISSN: 1110-1180
DOI: ---------

ERJ
Engineering Research Journal
Faculty of Engineering
Menoufia University

EFFECT of Dewatering System on Groundwater Contaminations Transport

Marwa Mohammed Mostafa[1], Esam Y. Helal[2], Mohamed F. Sobeh[3], Fahmy S. Abdelhaleem [4]

[1] *The holding company for drinking water and sanitation, Egypt*

[2, 3] *Civil Engineering Department, Faculty of Engineering, Menoufia University, Egypt*

[4] *Civil Engineering Department, Faculty of Engineering, Banha University, Egypt*

ABSTRACT

Deep excavation activities commonly require groundwater dewatering to lower the water table and construct different elements in normal conditions away from the groundwater table. The dewatering process changes the groundwater properties around the dewatering well area. This change includes the water table and water flow rate and subsequently causes contamination transport. This study discusses the relationship between dewatering and contamination spread in groundwater using a numerical model. The numerical modeling was performed by the 3D finite difference technique. The effects of various parameters were explored. These parameters included well depth, contamination depth, horizontal distance between the pollution source and the dewatering well, as well as contamination source discharge and the dewatering well discharge. The effects of the aforementioned parameters on contamination spread and contamination arrival time to the dewatering well area were discussed in the results. The results indicate that increase in both well and contamination depths increased contamination arrival time to dewatering well area and decrease in contamination spread. The effect of the pumping well on the contamination spread diminished when the horizontal distance exceeds twice of the aquifer depth. Also, the increase in pumping rate decreased the arrival time; conversely, the arrival time was extended by the increase in horizontal distance.

Keywords: *Groundwater; dewatering; contamination transport; numerical modelling.*

Introduction

Groundwater is better and more safe in many scenarios, than surface water because surface water is exposed more easily to pollutants from different sources. Lowering the groundwater level by pumping wells may reverse the normal flow of groundwater to the stream, causing the intrusion of surface water into groundwater and, eventually, drinking water wells [19]. It is very difficult and expensive to extract the pollutants from groundwater if it is polluted [3]. Efficient groundwater control provides safe construction of subsurface structures that are established beneath soil layers and under the water table. In choosing and constructing a dewatering method for the site of excavation, its depth, size, and form are essential variables [18]. Mansour [20] concluded that the hydraulic control can be effective in decelerating contamination migration. These pumping activities accelerate groundwater contamination transport. The effects of groundwater system contamination can continue even after the groundwater pumping stopped, as it takes a longer time for the aquifer to get back to its initial state [7]. Mozumder [22] performed a study demonstrating how local groundwater flow affects contamination across a range of time-scales. The study concluded that aquifers within the radius of influence of pumping wells expanded the Dhaka drawdown cone and magnified vertical and lateral head gradients determined by the heterogeneity in the local geology. This resulted in lateral transport of contamination through a major clay aquitard causing variable levels of the contamination in the study area. AbdElaty [1] investigated the impact of the coastal aquifers' boundary conditions change in light of climate change. The top layer criteria were evaluated on the basis of the erosion and sedimentation, irrigation, and drainage conditions, as well as factors representing the

upward brackish well parameters depending on the abstraction conditions. The SEAWAT model, which is a 3D model based on MODFLOW 2000, was used to simulate lateral sea water intrusion (SWI).The study recommended that to manage SWI, it is critical to monitor the saline water heads and groundwater recharge; the abstraction well should be used with a limited extraction rate, away from the coast, and with a short screen length. Using the computational models MODFLOW-NWT and MT3D-USGS, Schaper [26] predicted the transport of radioactive 222Rn during surface water penetration into an aquifer system. The study demonstrated that 222Rn transport can be properly modelled using open-source software tools MODFLOW-NWT and MT3D-USGS to minimize the uncertainty caused by sediment heterogeneity in transport times and increase the accuracy of transport time predictions. Allam [5] studied the effect of inclined barrier walls on the migration of contaminants across porous media. The results showed that the transport time was strongly affected by the inclination ratios of the barrier walls. Zhu [16] established a three-dimensional geological model of the Hougao area of the Dawu water source zone by summarizing and analyzing the hydrogeological data of the area. As an example of contaminants, ammonia nitrogen was chosen and the transport and diffusion of contaminant in the Hougao region was simulated. The study concluded that pollutants would rapidly spread to the centralized water supply region in the lack of any protection measures, posing a danger to the water supply. Ali [4] used a new grid-free semi-analytical integrated subsurface flow and reactive transport approach to investigate the impacts of vertical changes in permeability architecture and subsurface flow rate on sorption. According to the results, changes in the rate of vertical macro-scale heterogeneity in the subsurface permeability, including an exponential decrease in saturated hydraulic conductivity depth, can significantly affect subsurface sorption, the path of contaminants, and the time of stream arrival. Boddula [9] developed a new simulation model relying on Meshless Local PetrovGalerkin (MLPG) that predicts the groundwater head and concentration distribution in the study area. Also, the remediation system of contaminated groundwater aquifer via Pump and Treat is verified by coupling the Particle Swarm optimization model (PSO) with the simulation model for a hypothetical case study. Barilari [23] developed a hazard index (HI) to identify which point sources of groundwater contamination should be more regularly controlled and to recognize municipal supply wells that possibly be threatened. This (HI) index was applied to the city of Mar del Plata, Argentina. The HI is defined as the sum of 3 variables: Effluent Disposal mode (ED), Potential Contamination Load (PCL), and the distance from the point source to the groundwater wells or Well Protection Areas (WP). One of the groundwater pollution causes is the failed injection wells casings that result in the migration of fluids through the soil at injection depth [2]. Although injection wells are useful waste management techniques, the dangers connected with them are slightly understood, so knowledge is required to forecast the subsurface response to injection. The risk of contaminated potable groundwater is most concerned [15]. Wastes injected in the disposal site may interact with groundwater and minerals in the injection zone [10].

Previous studies explained the impact of contaminants spread and its various sources; the objective of this study is evaluating the effect of dewatering well depth, pumping rate, contaminated injection well depth and the horizontal distance between them on contaminations transport. Figure 1 shows an example of a field case where the polluted injection well became a source of contamination in the aquifer in which the dewatering system is constructed.

Theoretical background
Groundwater flow equation

The continuity equation expresses the groundwater flow. It explains the relationship between disturbances in the moisture content θ_w and the pressure head h and their impact on the water flow volumetric fluxes $\vec{q}$ in the flow domain [6].

$$\left(\frac{\partial \theta_w}{\partial h} + S\right)\frac{\partial h}{\partial t} = -\nabla \vec{q} \quad (1)$$

Where S is the specific storage coefficient and t is time. In the case of dewatering, the dewatering well effect should be taken in consideration so the continuity equation can be expressed:

$$S_s \frac{\partial h}{\partial t} = \frac{\partial}{\partial x_i}\left(K_{ii}\frac{\partial h}{\partial x_i}\right) + q_s \quad (2)$$

Where $K_{ii}$is the hydraulic conductivity, x_i is the distance along coordinate axis and $q_s$is the source/sink term that expresses the dewatering well [8]. In this study, the model domain will be an unconfined aquifer so q_s will be:

$$q_s = \frac{\pi K(H^2 - h_w{}^2)}{\ln R_0 / r_w} \quad (3)$$

where K is the hydraulic conductivity, H is the initial water head, h_w is the reduced water head after pumping, R_0 is called the radius of influence, beyond which there is no drawdown due to pumping and r_w is the radius of the pumping well [17].

Contaminations transport equation

The transport equation for groundwater is derived from the advection-dispersion equation. This derivation is governed by the law of the conservation of the mass of the solute flux in and out of a specific representative basic volume of porous media [12]. To apply this derivation, it must be assumed that the porous medium is isotropic, homogeneous, and saturated with water. The governing equation of a transported solute is:

$$\left[D_x \frac{\partial^2 C}{\partial x^2} + D_y \frac{\partial^2 C}{\partial y^2} + D_z \frac{\partial^2 C}{\partial z^2}\right] - \left[\mathrm{v_x} \frac{\partial C}{\partial x} + \mathrm{v_y} \frac{\partial C}{\partial y} + \mathrm{v_z} \frac{\partial C}{\partial z}\right] + q_s C_s = \frac{\partial C}{\partial t} \quad (4)$$

Where C is the solute concentration, v is average linear velocity, D is the hydrodynamic dispersion coefficient and C_s is the concentration of the sink/source flux [13].

When solutes move in groundwater they start to mix and disperse because of dispersion. Two types of dispersivity affect the spread of the contamination longitudinal and transverse dispersivity. Longitudinal dispersivity (α_l) is the spreading of the solute along the flow's longitudinal axis and the transverse dispersivity (α_t) is the mixing transverse to flow.

$\alpha_l = (0.83 * \log(l)^{2.41}) * 1.2\mathrm{m}$ (5)

$\alpha_t = 0.1 * \alpha_l \mathrm{m}$ (6)

Where l is flow path length [20].

Dimensional analysis

To investigate the problem and discover the relationship between parameters, the Buckingham π theorem was applied. The dimensionless relation was:

$$\mathrm{f}\left(\frac{\mathrm{d_1}}{\mathrm{D}}, \frac{\mathrm{d_2}}{\mathrm{D}}, \frac{\mathrm{X}}{\mathrm{D}}, \frac{\mathrm{L}}{\mathrm{D}}, \frac{\mathrm{Q}}{\mathrm{Q_0}}, \frac{\mathrm{T}}{\mathrm{T_0}}, \frac{\mathrm{C}}{\mathrm{C_0}}\right) = 0 \quad (7)$$

Where: T is the contamination arrival time, which represents the time the contamination takes to reach the pumping well with a concentration of 2% from the original contamination source concentration, T_0 is the total pumping time of the modelling = 100 days. d_1 is the contamination depth, d_2 is the dewatering well depth and the screens of both are 10 m high from the bottom of the wells. D is the aquifer depth and X is the horizontal distance between the dewatering well and the contamination. L is the spread distance of contamination, which is the distance the contamination transports toward the pumping well, starting at the contamination source and ending at the area with a 2% contamination concentration. Q is the pumping rate of the dewatering well, and Q_0 is the injection rate of the injection well and the groundwater level starts at the ground surface.

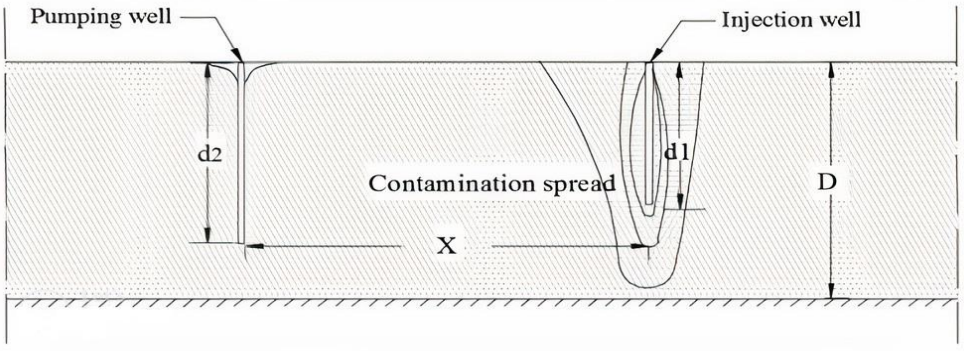

D= aquifer depth d_1=injection well depth
d_2= dewatering well depth X=distance between the dewatering and injection wells

Fig. 1 Cross-section shows the dewatering system and contamination source.

Numerical modelling

A 3D model was designed by applying the MODFLOW software to simulate the groundwater flow and direction, and the MT3DMS is used to simulate contamination transport. The wells are simulated using the (WELL) package that supported in VISUAL MODFLOW [7].

The dewatering system consists of a partially penetrating well with a pumping discharge Q and depth $\mathrm{d_2}$. The injection well also partially penetrates the aquifer with depth d_1 and distance X from the pumping well and injection rate $Q_0 = 1000 (m^3/d)$ with concentration $C_0 = 5000\ mg/l$. The total simulation time=100 days and hydraulic conductivity $K=10\ m/d$ (sand) [27]. The model domain consists of a homogeneous isotropic unconfined aquifer with depth $D = 100$ m and 3km^2 area with a rectangular shape and dimensions wider than the pumping well radius of influence to neglect the boundaries effect on the results. The lateral boundaries of the model are assumed to be constant head boundaries, and the

groundwater level starts at the ground surface. The modeling was performed considering the steady state, as the pumping rate and other input parameters were constant over time.

The aquifer numerical grid consists of 40 rows and 120 columns, and the vertical domain was divided into five layers. The model domain is shown in Figure (2) showing the meshing, boundary conditions and dimensions of the numerical model and Table (1) shows the numerical model input and Table (2) shows the Range of variable values used in the analysis including aquifer properties and basic input parameters required by the MT3DMS. The contamination spread during the model time at four consecutive time steps is shown in Figure (3).

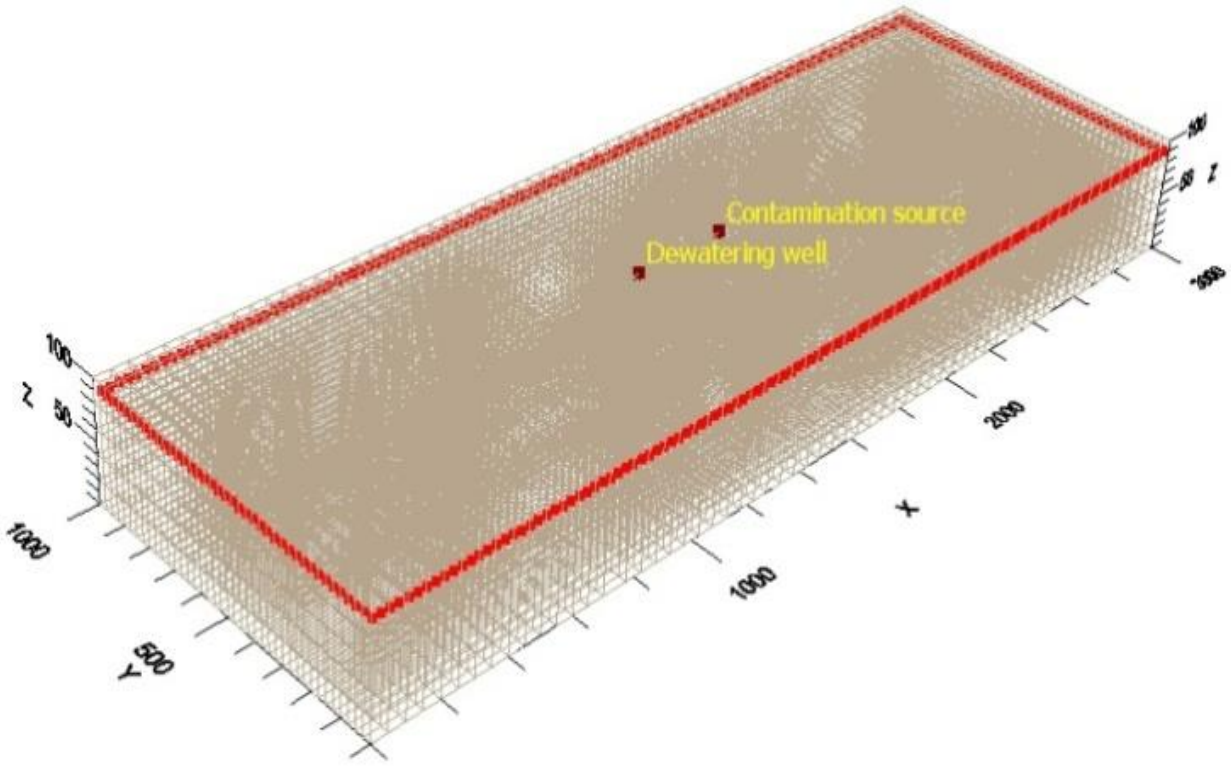

Fig. 2 3D view of the model grid.

Table 1: Input of the numerical model.

Aquifer depth *D*	100 m
Porosity (n)	0.3
Hydraulic conductivity (K)	10 m/d (sand)
Ratio between vertical and horizontal hydraulic permeability (k_x/k_y)	1.0
Mesh size	25 m
Time step	1 day

Table 2: Range of variable values used in the analysis

Distance between the dewatering and injection wells (X)	From 50 m to 300 m
Dewatering well depth (d_2)	From 20 m to 80 m
Injection well depth (d_1)	From 20 m to 80 m
Dewatering well discharge (Q)	From 2000 (m^3/d) to 10000 (m^3/d)

Wells with a depth of 20 meters are commonly used in construction dewatering, and wells with a depth of 80 meters are commonly used in mining dewatering [25].

The output parameters of the modeling are the contamination spread distance (L), final concentration at the pumping well area (C) and contamination arrival time (T).

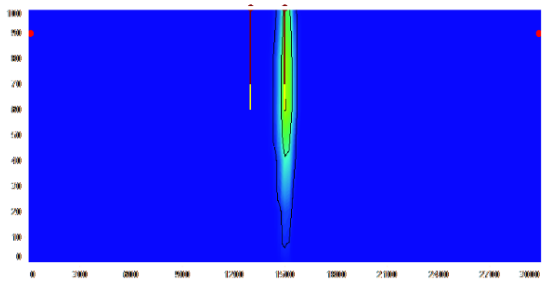

(a) Spread after 5 days of pumping.

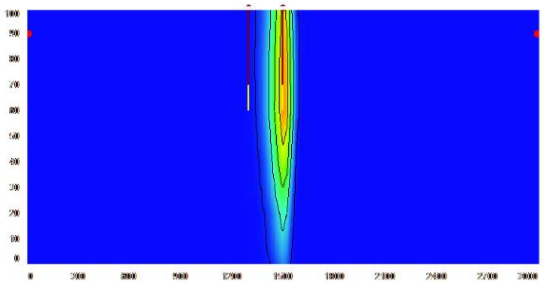

(b) Spread after 50 days of pumping.

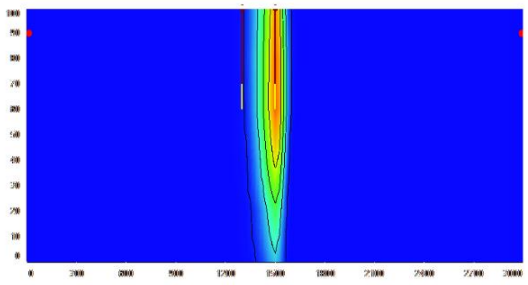

(c) Spread after 75 days of pumping.

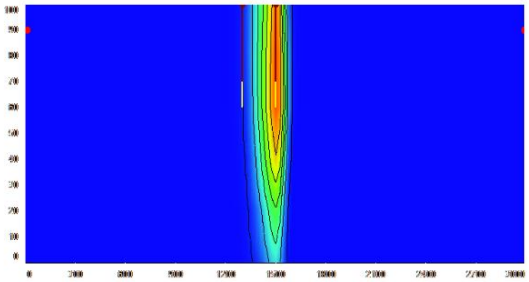

(d) Spread after 100 days of pumping.

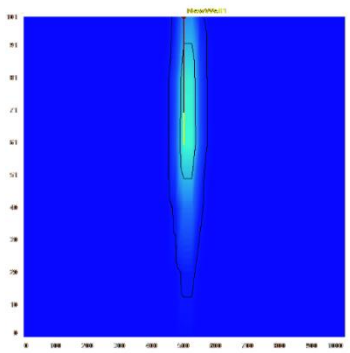

(e) The lateral spread of contamination in the transverse cross-section after 5 days of pumping.

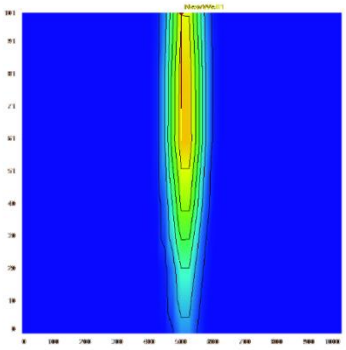

(f) The lateral spread of contamination in the transverse cross-section after 50 days of pumping.

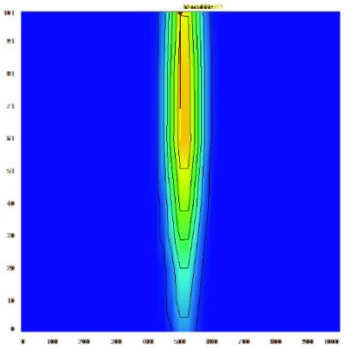

(g) The lateral spread of contamination in the transverse cross-section after 75 days of pumping.

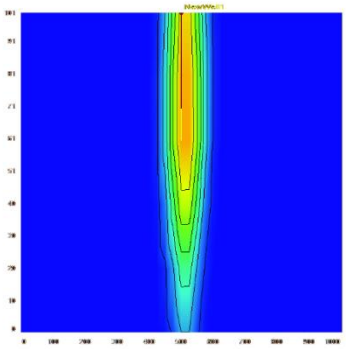

(h) The lateral spread of contamination in the transverse cross-section after 100 days of pumping.

Fig. 3 Contamination spread during modelling at (X/D=2, d_1/D=0.4, d_2/D=0.4, Q/Q_0=8 and after 100 d of pumping).

Results and analysis

The results for groundwater motion and hydraulics at (X/D=2, d_1/D=0.4, d_2/D=0.4, Q/Q_0=8 and after 50 days of pumping) are shown in **Figures 4 and 5.**

Fig. 4 shows the distribution of equipotential lines and groundwater heads for the mentioned case. The groundwater head around the well area equaled 95.1 m and the net flow rate was 50.00 m3/d. **Fig. 5** shows the flow paths, drawdown, directions and velocities. The maximum velocity = 12.881 m/d and the maximum drawdown =4.9 m. The direction and velocities are represented by the arrows toward the pumping well screen.

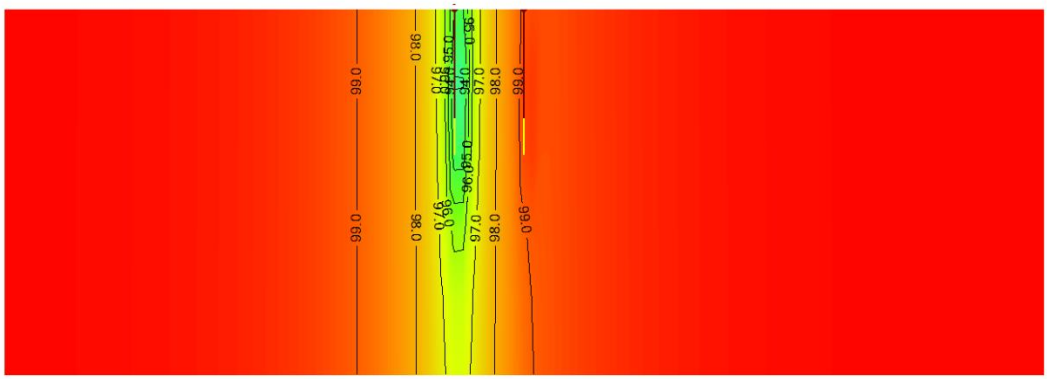

Fig. 4 Distribution of equipotential lines and groundwater head.

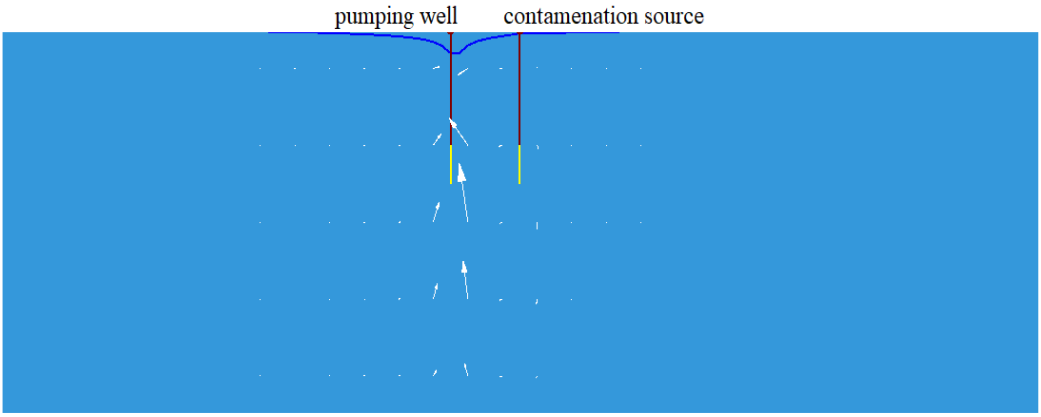

Fig. 5 Groundwater table and velocities.

The results shown in **Figures 6–13** considered an arrival time of 2% concentration to the dewatering well area. The contamination flux and spread increased due to the increase in relative pumping rate, according to eq. 4, which agrees with the results of Mozumder [22], and for the same pumping rate, the spread at small horizontal distances between the well and contamination is relatively small because the contamination reaches the pumping well rapidly and being pumped by the pumping well so its spread became limited counter to spread at wide distances that take a longer time to reach the well and being pumped **Fig. 6.** The relative solute concentration is inversely proportional to the relative distance between the well and the contamination according to eq. 4.

The effect of the pumping well on the contamination spread diminished when the horizontal distance (X) exceeds twice of the aquifer depth **Fig. 7.**

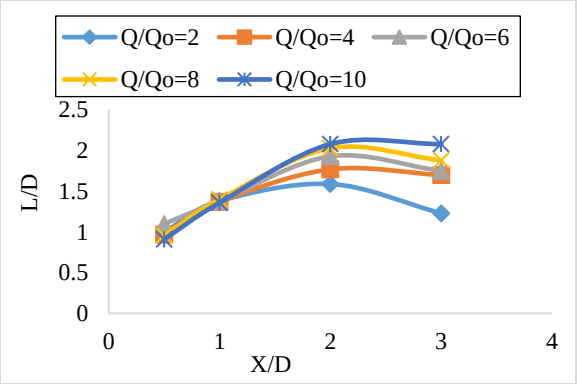

Fig. 6 Effect of horizontal distance on contamination spread at d_2/D=0.4 and d_1/D=0.4 after 100 d of pumping, the concentration varies with each case.

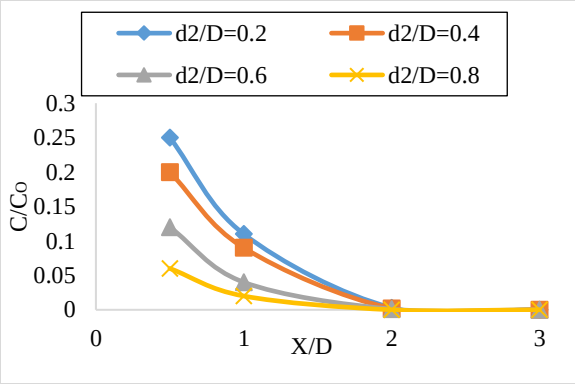

Fig. 7 Effect of horizontal distance on final concentration at dewatering well at Q/Q_0=2 and d_1/D=0.8 after 100 d of pumping.

The dewatering well depth, contamination depth, distance between the well and the contamination, and dewatering pumping rate are considered the main factors that control the contamination arrival time at the pumping well area. **Fig. 7** shows the decrease in concentration with the increase in pumping well depth, which occurs when the contamination source is relatively deep (in this case d_1/D= 0.8). When the pumping well is relatively shallow, the deep contamination takes a long time to reach to the pumping well and is then the pumping well pumps it out of the ground, resulting in a high final concentration. However, when the pumping well is relatively deep, the deep contamination takes a shorter time to reach the pumping well and is then pumped out of the ground, resulting in a lower final concentration.

Fig. 8 shows that for higher values of relative depth of the pumping well d_2/D the effect of increasing contamination depth d_1/D is significant on T/T_0 for higher values of d_2/D and decreased with lower values of d_2/D. Increasing depths of pumping well or contamination source led to increasing the arrival time this is because the path travelled by contamination increases and that agrees with Chen [13].
Increasing the pumping well depth effect on the arrival time, for (d_1/D) = 0.4 and 0.2 curves the effect is weak but it start to be significant with depths (d_2/D) = 0.6 and 0.8 because of the increase in path length [24].

Fig. 9 shows that for lower relative horizontal distance between pumping well and contamination an increase in d_2/D led to a slight increase in T/T_0. The effect is significant for higher values of X/D.

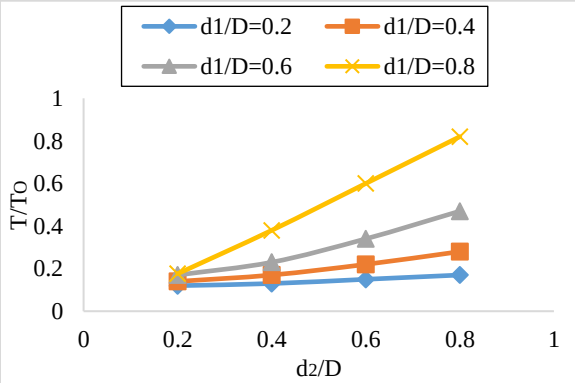

Fig. 8 Effect of dewatering well depth on contamination arrival time at Q/Q_0=6 and X/D=1 and the concentration varies with the variation of pumping well depth and contamination depth.

Fig. 10 shows that an increase in d_1/D increased T/T_0 and this effect is much significant with higher values of d_2/D. Also, the increase in d_2/D led to increase in $T/T_0$with a more notable effect for higher values of d_2/D than lower values and this is due to increase in contamination path length that increases with increase in depth [24]. This happens because the distance the contamination travels increases with the increase in X/D and d_2/D and the travelled distance is conversely proportional to the arrival time.

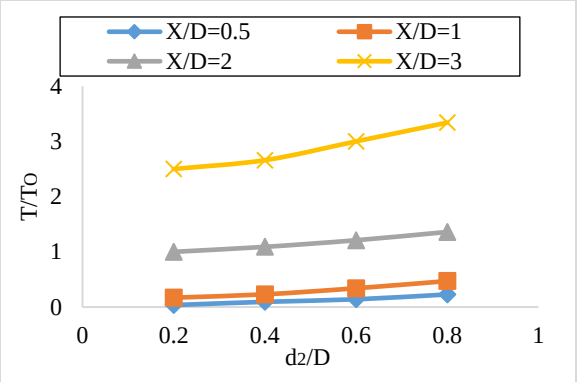

Fig. 9 Effect of dewatering well depth on contamination arrival time at d_1/D=0.6 Q/Q_0=6 and the concentration varies with the variation of pumping well depth and horizontal distance. The total pumping time is 100 d and the arrival time is different for each case.

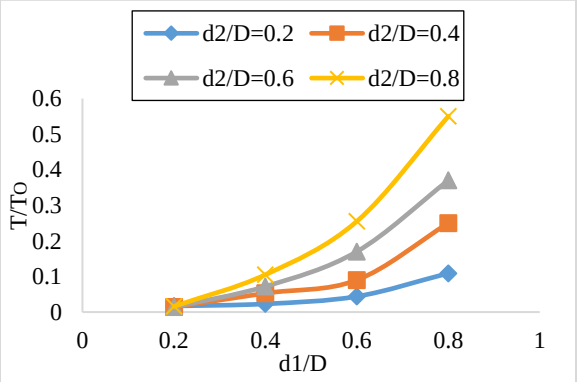

Fig. 10 Effect of contamination depth on arrival time at Q/Q_0=2 and X/D=0.5 and the final concentration varies with variation of pumping well and contamination depths. The total pumping time is 100 d and the arrival time is different for each case.

Fig. 11 shows that for higher values of relative horizontal distance between the pumping well and contamination X/D, the arrival time is relatively high. Increasing the relative dewatering pumping rate led to decreasing in the arrival time this is because the arrival time is inversely proportional to groundwater flux [13].

Fig. 12 shows the decrease of T/T_0 as Q/Q_0 increases because the arrival time is inversely proportional to groundwater flux as mentioned before and increasing the relative depths of contamination source led to increasing in relative arrival time as the path length increases [22].

Fig. 13 shows the decrease of contamination spread distance L/D as d_1/D increases, also increasing the pumping well depth led to decrease in contamination spread. This happens because the contamination flux is inversely proportional to vertical depth, as mentioned in eq. 4.

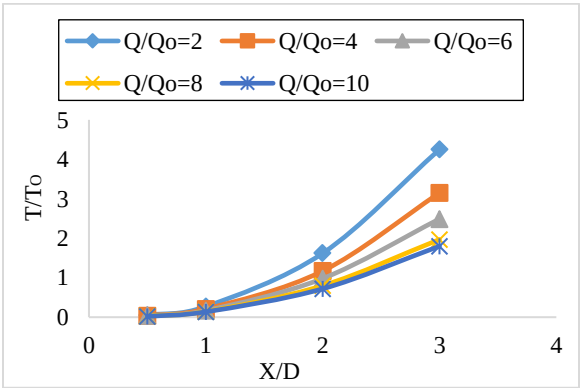

Fig. 11 Effect of horizontal distance on contamination arrival time at d_2/D=0.4 d_1/D=0.4 the final concentration varies with the variation of horizontal distance and pumping rate. The total pumping time is 100 d and the arrival time is different for each case.

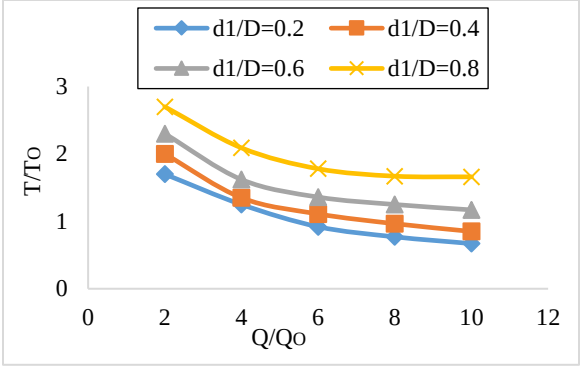

Fig. 12 Effect of pumping rate on contamination arrival time at X/D =2 and d_2/D =0.8 and the concentration varies with the variation of pumping well depth and pumping rate.
The total pumping time is 100 d and the arrival time is different for each case.

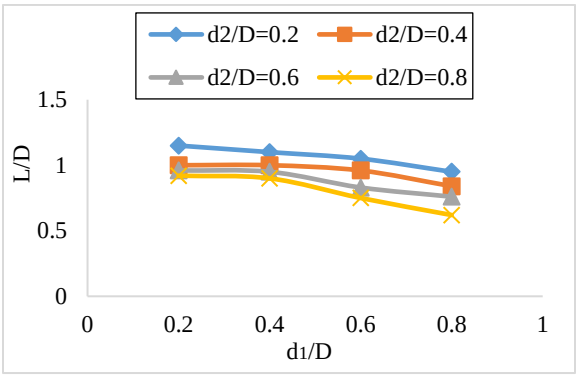

Fig. 13 Effect of contamination depth on contamination spread at Q/Q_0=2 and X/D =0.5 after100 d of pumping and the concentration varies with each case.

Fig. 14 shows the decrease in the contamination spread distance L/D as d_2/D increases as the contamination flux is inversely proportional to vertical depth as mentioned in eq. 4 that agree with the results of [1]. Also the contamination spread decreases with the increase in contamination source depth.

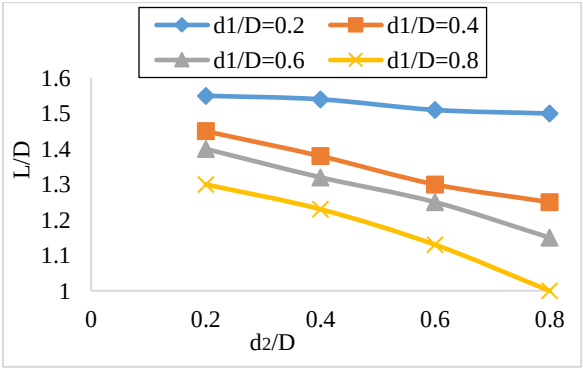

Fig. 14 Effect of dewatering well depth on contamination spread at Q/Q_0= 6 and X/D=1 after 100 d of pumping and the concentration varies with each case.

Conclusions

A 3D groundwater flow and contamination transport models were applied to study the effect of groundwater dewatering on contamination transport in an aquifer. The numerical modelling was carried out using MODFLOW software with both the WELL and MT3DMS packages. The study focused on 4 parameters affecting the contamination transport: these parameters are pumping discharge rate, horizontal distance between the pumping well and the contamination source, pumping well depth, and contamination source depth. The effect of the pumping well on the contamination spread diminished when the horizontal distance (X) exceeds twice of the aquifer depth. Increasing both of dewatering well depth and contamination source depth led to increasing in contamination arrival time to dewatering well. The depths of the dewatering well and contamination source were basic parameters, which affected the arrival of the contamination. Also, increasing the horizontal distance between the pumping well and contamination source increased the arrival time; however, increasing the pumping rate of the dewatering well lad to decrease in the arrival time. A decrease in contamination spread distance happened because of contamination depth increase and dewatering well depth increase.

References

1. AbdElaty, et al., 2022. "Sustainable management of two-directional lateral and upcoming saltwater intrusion in coastline aquifers to alleviate water scarcity," Hydrological processes.
2. Akob, et al., 2016. "Wastewater disposal from unconventional oil and gas development degrades stream quality at a West Virginia injection facility," Environmental science & technology, 50 (11), pp. 5517-5525.
3. Alexander Zaporozec, 2004. "Groundwater contamination inventory," UNESCO.
4. Ali A. Ameli, 2017. "Controls on subsurface transport of sorbing contaminant," Hydrology research, vol 48, No. 5, PP. 1226- 1239.
5. Allam, et al., 2019. "Retarding contaminant migration through porous media using inclined barrier walls," Journal of hydrology and hydromechanics, 67(4), pp.339-348.
6. Allen, et al., 1989. "Intermedia pollutant transport," National center for intermedia transport research (U.S.)
7. Bedekar, et al., 2016. "MT3D-USGS version 1: A U.S. geological survey release of MT3DMS updated with new and expanded transport capabilities for use with MODFLOW," U.S. geological survey techniques and methods 6-A53, 69 p.
8. Bergvall, et al., 2011. "Modeling subsurface transport in extensive glaciofluvial and littoral sediments to remediate a municipal drinking water aquifer," Hydrology and earth system sciences, 15(7), pp.2229-2244.
9. Boddula, Eldho, 2016. "Simulation-optimization models for the remediation of groundwater contamination," Geo-Chicago, vol. 273, PP. 381-391.
10. Brower, et al., 1989. "Evaluation of underground injection of industrial waste in Illinois," Champaign, Ill.: Illinois state geological survey.
11. Chapman, D., 2007. "Water quality assessments," London: E & FN Spon.
12. Charles R. Fitts, 2013. "Groundwater science (Second edition)," Academic press.
13. Chen, Z., et al., 2006. "Computational methods for multiphase flows in porous media," Norwich, NY: Knovel.
14. Duriez, 2005. "On the use of groundwater contaminant transport modelling in risk assessments," Chalmers University of technology, Sweden.
15. Ferguson, G., 2014. "Deep injection of waste water in the Western Canada sedimentary basin," Groundwater, 53(2), pp.187–194.
16. Henghua Zhu, et al., 2019. "Control effects of hydraulic interception wells on groundwater pollutant transport in the Dawu water source area," Water, vol.11, PP.1-18.
17. Powers, et al., 2007. "Construction dewatering and groundwater control: New methods and applications, Third edition," John Wiley & sons, Inc.
18. Wickham, Gabriel, 1985. "Dewatering and groundwater control," Washington: Departments of the army, the navy, and the air force.
19. Malaguerra, et al., 2013. "Assessment of the contamination of drinking water supply wells by pesticides from surface water resources using a finite element reactive transport model and global sensitivity analysis techniques," Journal of hydrology, 476, pp.321-331.
20. Mansour, et al., 2018. "Delaying solute transport through the soil using unequal double sheet piles with a surface floor," Ain Shams engineering journal, 9(4), pp.3399-3409.
21. Mathes, et al., 2002. "Geographic information systems (GIS) mapping of groundwater

contamination at the Savannah River site (SRS)," The university of Georgia.

22. Mozumder, et al., 2020. "Origin of groundwater arsenic in a rural pleistocene aquifer in Bangladesh depressurized by distal municipal pumping," Water resources research, 56(7).
23. Mustafa et al., 2020. "Solute transport modelling to manage groundwater pollution from surface water resources," Journal of contaminant hydrology, vol. 233.
24. Ophori, et al., 1998. "Hydrologic response to pumping and contaminant advection in a fractured rock environment," Journal of the American water resources association, 34(1), 57–72.
25. Rozkowski, et al., 2021. "Open-pit mine dewatering based on water recirculation-case study with numerical modelling," Energies.
26. Schaper, et al., 2022. "Spatial variability of Radon production rates in an alluvial aquifer affects travel time estimates of groundwater originating from a losing stream," Water resources research, 58(4).
27. Shackelford, 2013. "Reference module in earth systems and environmental sciences," Geoenvironmental engineering.